Support Information

Wenqi Zhao, Minghui Cui, Yansong Zhou, Yanjing Liu, Qiongrong Ou[*]*, Shuyu Zhang*[*]

State Key Laboratory of Photovoltaic Science and Technology, Institute for Electric Light Sources, School of Information Science and Technology, Fudan University, Shanghai, 200433, China.

E-mail addresses: qrou@fudan.edu.cn (Q. Ou), zhangshuyu@fudan.edu.cn (S. Zhang).

[*]Qiongrong Ou. E-mail address: qrou@fudan.edu.cn

[*]Shuyu Zhang. E-mail address: zhangshuyu@fudan.edu.cn

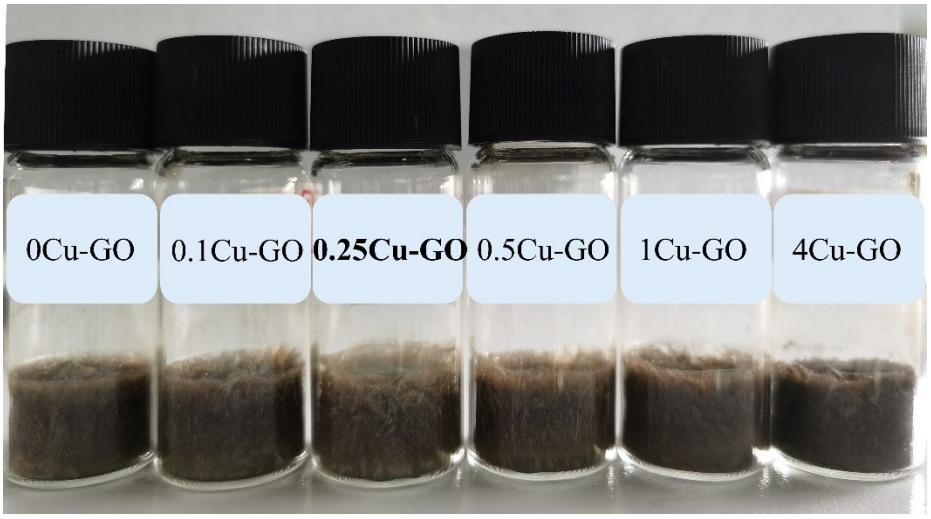

Fig. S1. Digital photo of freeze-dried xCu-GO with the same volume of solution.

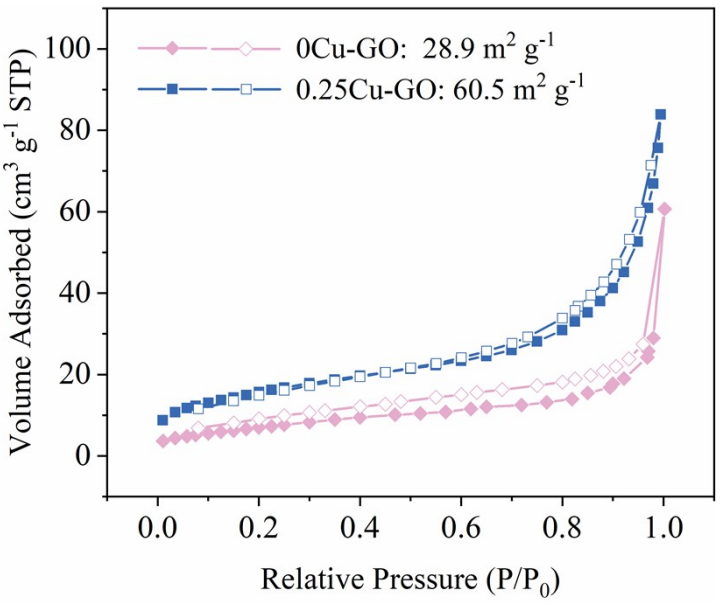

Fig. S2. N_2 adsorption-desorption isotherms of 0Cu-GO and 0.25Cu-GO.

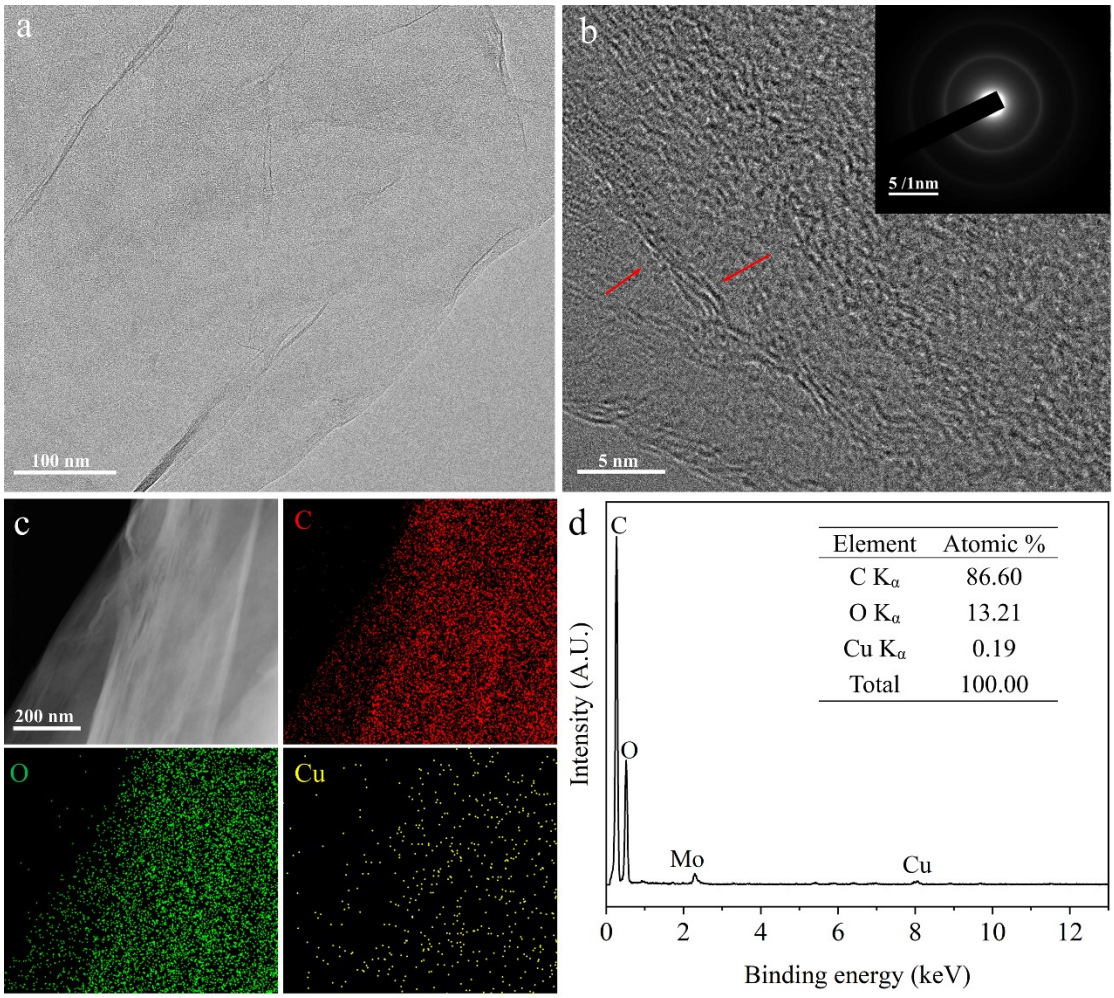

Fig. S3. (a) TEM image of 0.25Cu-GO. (b) HRTEM image of 0.25Cu-GO (the inset in b is the SAED pattern). (c) High-angle annular dark-field scanning transmission electron microscopy (HAADF-STEM) image and the corresponding elemental mapping of 0.25Cu-GO. (d) EDX spectrum measured during TEM analysis.

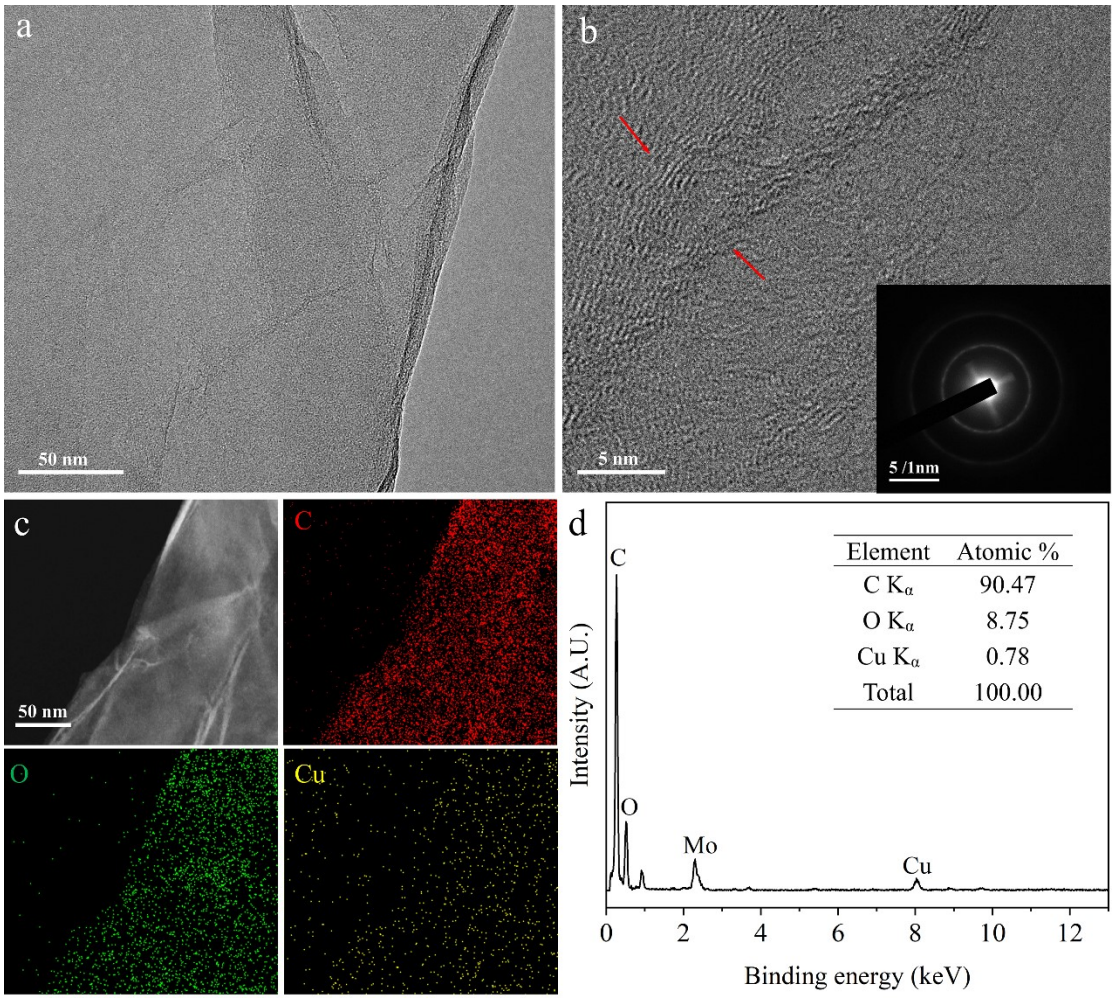

Fig. S4. (a) TEM image of 4Cu-GO. (b) HRTEM image of 4Cu-GO (the inset in b is the SAED pattern). (c) HAADF-STEM image and the corresponding elemental mapping of 4Cu-GO. (d) EDX spectrum measured during TEM analysis.

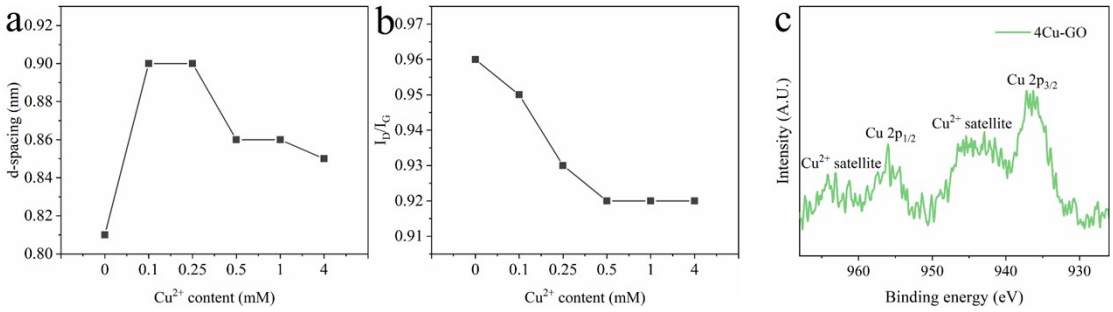

Fig. S5. (a) d-spacing of xCu-GO as a function of Cu^{2+} content. (b) The I_D/I_G value of xCu-GO Raman spectra as a function of Cu^{2+} content. (c) Cu 2p XPS spectra of 4Cu-GO.

Table S1. Components of C1s spectra of 0Cu-GO and 0.25Cu-GO (relative atomic percentage %)

	C	O	C-C/C=C	C-O	C=O	O-C=O
0Cu-GO	67.4	32.6	43.9	47.2	5.7	3.2
0.25Cu-GO	69.5	30.5	47.3	44.8	5.4	2.5

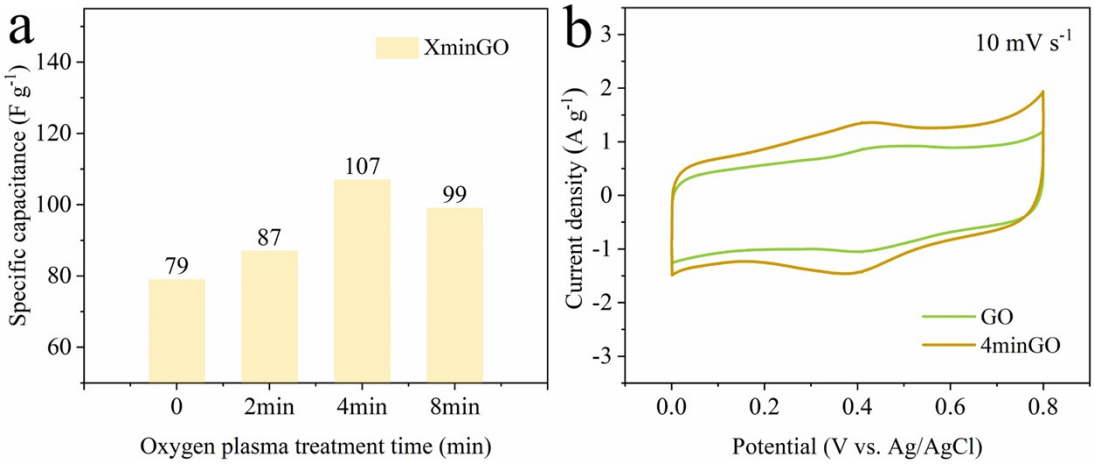

Fig. S6. (a)The specific capacitance at 1.5 A g^{-1} for XminGO. (b) CV curves of GO and 4minGO at 10 mV^{-1}.

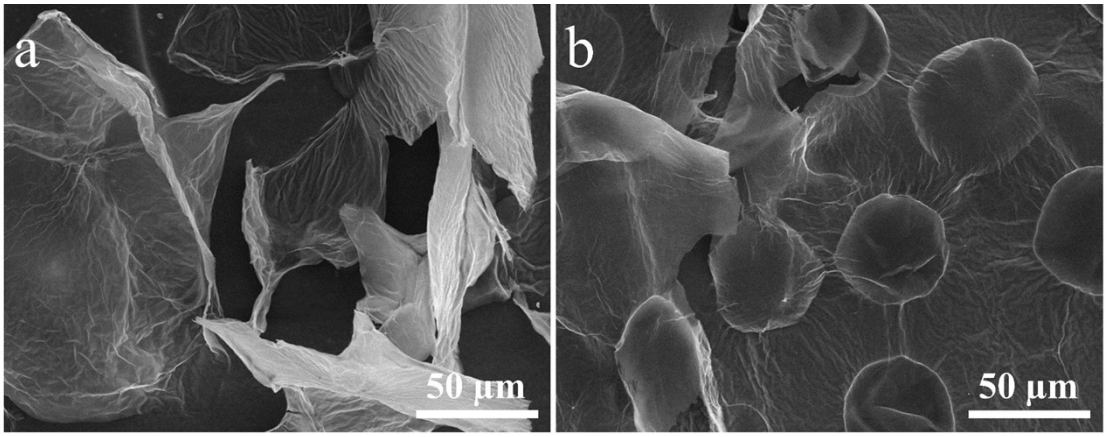

Fig. S7. SEM images of (a) 4minGO, and (b) 8minGO.

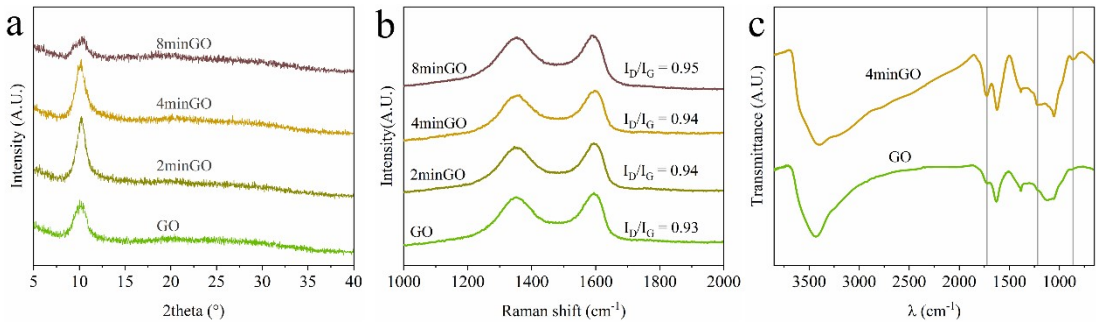

Fig. S8. (a) XRD patterns of XminGO. (b) Raman spectra of XminGO. (c) FTIR spectra of GO and 4minGO.

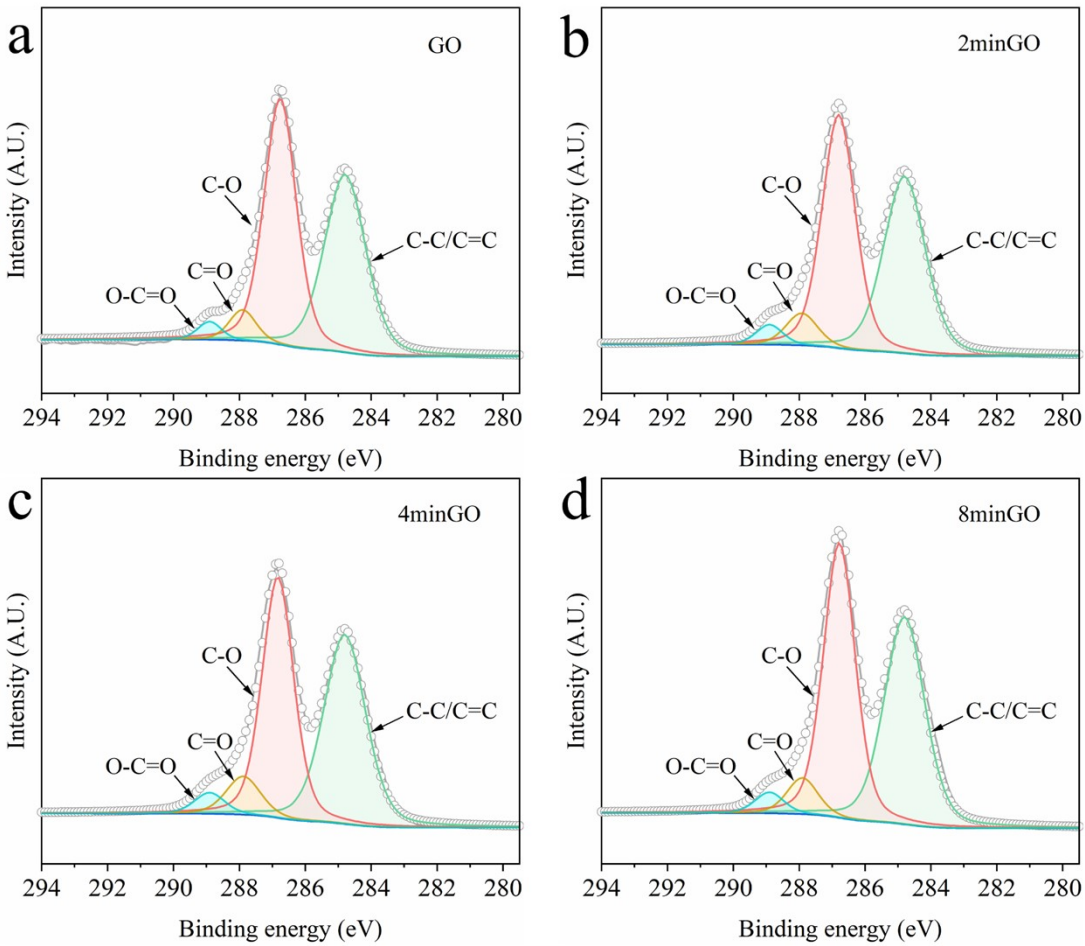

Fig. S9. C 1s XPS spectra of (a) GO, (b) 2minGO, (c) 4minGO, and (d) 8minGO.

Table S2. Components of C1s spectra of XminGO (relative atomic percentage %)

	C	O	C-C/C=C	C-O	C=O	O-C=O
GO	66.3	33.7	43.4	48	5.7	2.9
2minGO	67	33.1	44.1	46.6	6.1	3.2
4minGO	67.6	32.6	45.4	43.5	7.5	3.6
8minGO	67.9	32.1	44.5	46.4	5.9	3.2

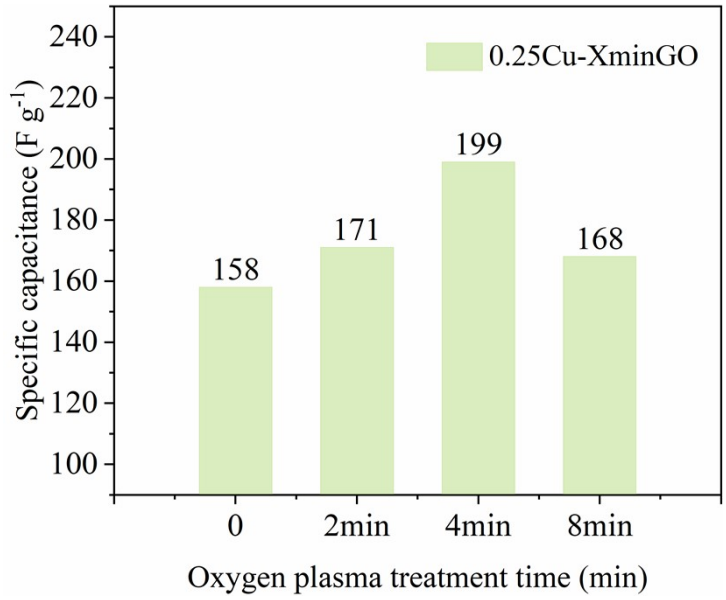

Fig. S10. The specific capacitance at 1.5 A g^{-1} for 0.25Cu-XminGO.

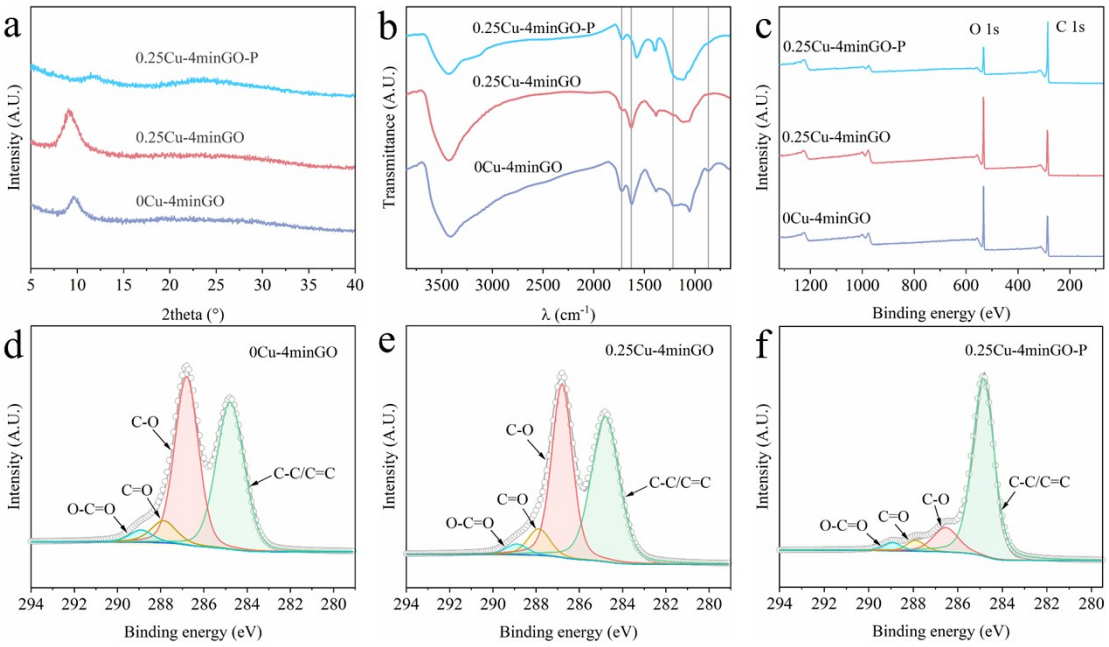

Fig. S11. (a) XRD patterns of 0Cu-4minGO and 0.25Cu-4minGO/0.25Cu-4minGO-P. (b) FTIR spectra of 0Cu-4minGO and 0.25Cu-4minGO/0.25Cu-4minGO-P. (c) XPS survey spectra of 0Cu-4minGO and 0.25Cu-4minGO/0.25Cu-4minGO-P. C 1s XPS spectra of (d) 0Cu-4minGO, (e) 0.25Cu-4minGO, and (f) 0.25Cu-4minGO-P.

Table S3. Components of C1s spectra of (relative atomic percentage %) 0Cu-4minGO and 0.25Cu-4minGO/0.25Cu-4minGO-P

	C	O	C-C/C=C	C-O	C=O	O-C=O
0Cu-4minGO	68.7	31.3	45.3	44.2	7.1	3.4
0.25Cu-4minGO	69.1	30.9	47.9	42.4	7.0	2.7
0.25Cu-4minGO-P	83.2	16.8	81.6	12.2	3.2	3.0

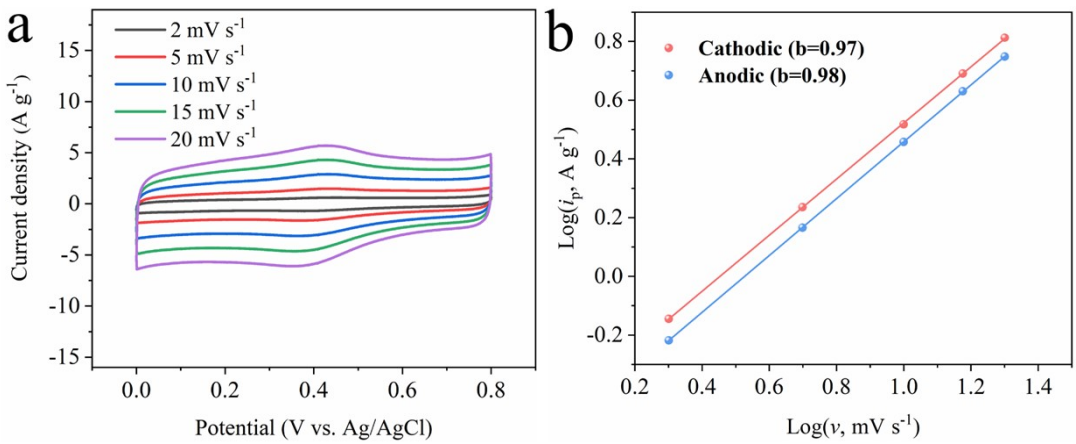

Fig. S12. (a) CV curves of 0.25Cu-4minGO-P at different scan rates. (b) The fitting plots between log(*i*) and log(*v*) of the redox peaks around 0.4 V.

The electrochemical reaction kinetics of the material is investigated according to the equation: $i_p = av^b$, where i_p is the peak current (A), v is the scan rate ($mV \cdot s^{-1}$), and a and b are constants. By fitting plots between log(*i*) and log(*v*) at low scan rates, as Fig. S12 shows, the b values of the redox peaks are calculated to be approximately 1, which indicates a capacitive-controlled mechanism during the charge storage process.

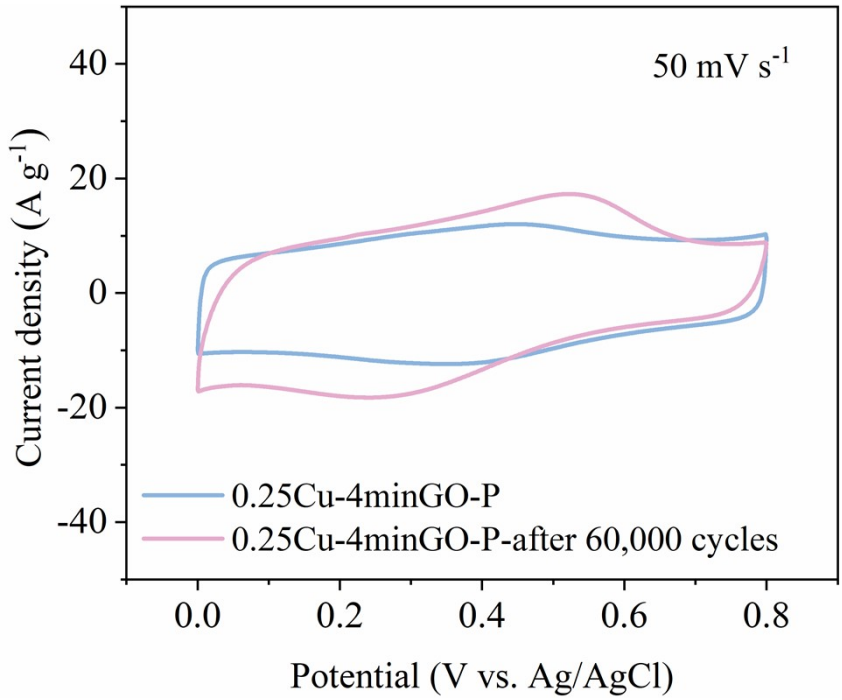

Fig. S13. CV curves of 0.25Cu-4minGO-P and after 60,000 cycles at 50 mV s^{-1}.

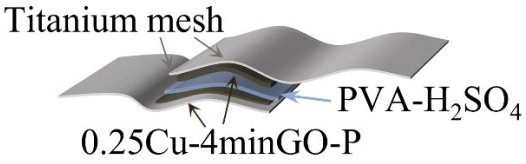

Fig. S14. Schematic illustration of an all-solid-state symmetric supercapacitor.